Increased level of FAM19A5 is associated with cerebral small vessel disease and leads to a better outcome

Zhongnan Hao[1], Shaonan Yang[1], Ruihua Yin[1], Jin Wei[1], Yuan Wang[1], Xudong Pan[1], and Aijun Ma[1]

[1]Department of Neurology, The Affiliated Hospital of Qingdao University, Medical School of Qingdao University, Qingdao, Shandong Province, China

Corresponding authors:

Xudong Pan[1] and Aijun Ma[1]

59 Haier Road, Qingdao, Shandong Province, 266100, China.

E-mail addresses: drpan055@163.com (X. Pan), drmaj@126.com (A. Ma)

27

Abstract:

Objective. FAM19A5 plays an essential role in the development and acute or chronic inflammation of the central nervous system. The present study aimed to explore the association between FAM19A5 and cerebral small vessel disease (cSVD).

Methods. A total of 344 recent small subcortical infarct (RSSI) patients and 265 healthy controls were included in this study. The difference in the FAM19A5 level between the two groups was compared and the correlation between FAM19A5 and cerebral infarction volume was analyzed. Also, the association between FAM19A5 and the total magnetic resonance imaging (MRI) burden with its imaging characteristics was explored. Moreover, the correspondence of FAM19A5 with the outcome was assessed via Δ National Institutes of Health Stroke Scale score (NIHSS) and the percentage of NIHSS improvement.

Results. FAM19A5 was highly expressed in the RSSI group (P=0.023), showing a positive correlation with cerebral infarction volume (P<0.001). It was positively correlated with total MRI cSVD burden (P<0.001) and reflected the severity of white matter hyperintensity (WMH) (P<0.001) and enlarged perivascular space (EPVS) (P<0.001), but did not show any association with cerebral microbleed (CMB) and lacune. Moreover, FAM19A5 suggested a larger ΔNIHSS (P=0.021) and NIHSS improvement percentage (P=0.007).

Conclusion. Serum FAM19A5 was increased in RSSI and positively correlated with the infarct volume. It also reflects the total MRI burden of cSVD, of which the imaging characteristics are positively correlated with WMH and EPVS. In addition, higher FAM19A5 levels reflect better outcomes in RSSI patients.

49

1. Introduction

Recent small subcortical infarction (RSSI), formerly known as lacunar infarct, accounts for 25% of all acute ischemic strokes. It results from the occlusion of a minor, single perforating brain artery, supplying subcortical areas in the deep white matter, basal ganglia (BG), thalamus, or pons (Cannistraro et al. 2019; Gattringer et al. 2015). Typically, the core mechanism of cSVD-related brain acute injury is considered to be ischemia, which effectuates through arteriolar stenosis or occlusion, irrespective of structural or functional (such as vasospasm, impaired self-regulation, or hypotension) (Wardlaw et al. 2013a). RSSI is one of the critical MRI characteristics of cerebral small vessel disease (cSVD). Lacune, white matter hyperintensity (WMH), enlarged perivascular

59 space (EPVS), and cerebral microbleed (CMB) are also components of cSVD imaging
60 characteristics (Wardlaw et al. 2013b). The main symptoms of cSVD are stroke (subcortical
61 infarction and cerebral hemorrhage), cognitive and affective disorders, gait disorder, and overall
62 function decline. The pathogenesis of cSVD is complicated; various MRI imaging characteristics
63 and different parts of lesion sites show unique pathogenesis that is independent and interrelated
64 (Blanco et al. 2017; Satizabal et al. 2012; Wardlaw et al. 2013a).

65 FAM19A5, also known as TAFA-5, belongs to the family with sequence similarity 19 comprising
66 five highly homologous genes (*FAM19A1-5*) (Tom Tang et al. 2004). Using X-gal staining in
67 FAM19A5-LacZ knock-in mice, a previous found that FAM19A5 participates in the nervous
68 system development from an early stage, expresses in neurons, oligodendrocyte precursor cells
69 (OPCs), astrocytes, and microglia. Also, using the traumatic brain injury (TBI) model, FAM19A5
70 is suggested to be involved in the OPC-mediated repair process as an acute inflammatory factor
71 after pathological brain injury(Shahapal et al. 2019). The participation of FAM19A5 in the TNF-
72 α-induced hypothalamus inflammatory response also confirmed the role of FAM19A5 in acute
73 inflammation (Kang et al. 2020). Moreover, as a bridge connecting chronic inflammation, reactive
74 gliosis, and degenerative diseases in the brain, FAM19A5 is overexpressed in severe depressive
75 disorder, Alzheimer's, Parkinson's disease, and vascular dementia (Han et al. 2020; Li et al. 2020;
76 Li et al. 2021; Mez et al. 2017).

77 Several studies demonstrated that inflammation plays a crucial role in the pathogenesis of cSVD
78 (Blanco et al. 2017; Kwee & Kwee 2007; Satizabal et al. 2012; Wardlaw et al. 2013a); whether
79 FAM19A5 affects the pathogenesis of cSVD as an inflammatory factor has not yet been published.
80 Based on the association among laboratory, imaging, and clinical assessments, the present study
81 aimed to explore the correlation between FAM19A5 and cSVD.

82

83 2. Methods

84 2.1. Subjects

85 Cerebral infarction patients and healthy individuals admitted to the Institute of Cerebrovascular
86 Diseases Cooperative Medical Institutions from May 2018 to June 2020 were continuously
87 enrolled in this study. RSSI is defined as a recent deep small infarction caused by a single
88 perforating artery occlusion, leading to ischemic necrosis of the brain tissue in its blood supply
89 area. The inclusion criteria were as follows: RSSI patients showing typical cerebral infarction
90 symptoms and physical signs with ischemic focus <20 mm in brain MRI. The exclusion criteria
91 were as follows: patients with carotid or intracranial artery stenosis >50%, cardiogenic stroke,
92 previous cardiocerebrovascular disease, severe liver or kidney function injury, and inflammation-

93 related diseases, such as rheumatic immune disease and tumor. This study was conducted
94 following the Declaration of Helsinki, was approved by the Ethics Review Board of the Affiliated
95 Hospital of Qingdao University (QYFY WZLL 26787), and informed consent was taken from all
96 individual participants.

2.2. Clinical analysis of subjects

98 Data, including age, sex, vital signs (blood pressure and pulse), history (hypertension and
99 diabetes), personal history (smoking and drinking history), and basic laboratory examinations
100 (glucose, triglyceride, total cholesterol, low-density lipoprotein, high-density lipoprotein, white
101 blood cell count, and uric acid), were collected from medical records of all the subjects at the time
102 of registration. All the healthy controls underwent electrocardiography (ECG) and brain imaging
103 examinations (head computed tomography (CT) scan or head MR scan), while the RSSI patients
104 received the following examinations: cerebral MRI, carotid artery examination, and
105 cerebrovascular examination (arterial CTA or MRA), cardiac ultrasound, and 24-h Holter
106 electrocardiogram. A total of 146 RSSI patients completed the head susceptibility-weighted
107 imaging (SWI) examination. RSSI patients underwent laboratory examinations with respect to C-
108 reactive protein, high sensitivity C-reactive protein, and homocysteine. We also evaluated the
109 patients' NIHSS score at admission and 14 days and calculated ΔNIHSS (NIHSS at
110 admission−NIHSS at 14 days) and percentage of NIHSS improvement ((NIHSS at
111 admission−NIHSS at 14 days)/NIHSS at admission). Also, the total MRI burden of patients in the
112 RSSI group was estimated.

2.3. Serum analysis for FAM19A5 levels

114 Fasting blood was withdrawn within 24 h of admission, and the serum was collected by
115 centrifugation at $1,000 \times g$ for 15 min and stored at −80 ℃. The serum FAM19A5 level of all
116 patients was determined by a double sandwich enzyme-linked immunosorbent assay kit (Jonln
117 Biology, Wuhan, China), with inter-assay CV% < 10%, and intra-assay CV% < 15%, using 50 μL
118 of each sample with no sample dilution. We strictly follow the operating instructions: the standard,
119 specimen, and HRP-conjugate detection antibody were added to the microwells pre-coated with
120 the FAM19A5 capture antibody in sequence. After incubation and washing thoroughly, the color
121 was developed by TMB, and the optical density was measured at 450 nm on a microplate reader
122 (Molecular Devices, San Jose, CA, USA).

2.4. Radiological assessment

124 All RSSI patients were examined using 3.0T MRI, and the images were read and analyzed by two
125 professional neurologists; any differences were resolved through discussion with a third analyst.
126 The volume of cerebral infarction was calculated using the ABC/2 method (Sims et al. 2009). Each
127 imaging characteristic of the cSVD (WMH, EPVS, lacune, CMB) was evaluated separately. The

128   lacune of presumed vascular origin has defined as a round or ovoid, subcortical, fluid-filled cavity
129   (signal similar to CSF) between 3 mm and 15 mm in diameter, consistent with a previous acute
130   small subcortical infarct or hemorrhage in the territory of one perforating arteriole. EPVS has
131   defined as fluid-filled spaces that follow the typical course of a vessel as it goes through grey or
132   white matter. The spaces have a signal intensity similar to CSF on all sequences. According to
133   Potter scale, we counted the number of enlarged perivascular spaces and divided them into 0, 1, 2,
134   3, and 4 grades (0, 1–10, 11–20, 21–40, ≥40, respectively) (Potter et al. 2015). WMH has been
135   defined as a signal abnormality of variable size in the white matter that shows the following
136   characteristics: hyperintensity on T2-weighted images (T2WI) such as fluid-attenuated inversion
137   recovery without cavitation (signal different from CSF); WMH was divided into periventricular
138   WMH (PVWMH) and deep WMH (DWMH) that were graded by Fazekas scale, respectively
139   (Wardlaw et al. 2013b), Only RSSI patients with head SWI were evaluated for CMB, which was
140   defined as a small focal round lesion (diameter <10 mm), showing a low signal on SWI. The CMB
141   was classified into lobar CMB and deep CMB. The presence of lacune, the presence of CMB, the
142   number of EPVS ≥11, Fazekas scale ≥2, and each parameter assessed as one score were included
143   in the total MRI burden of cSVD.

144   **2.5. Statistical analysis**

145   The normality of quantitative data distribution was assessed using the Kolmogorov– Smirnov test.
146   Continuous variables with normal distribution were described as mean±standard deviation (SD),
147   continuous variables with non-normal distribution were described as median (interquartile range
148   (IQR)), and qualitative data were described as quantity (percentage). Multivariable logistic
149   regression analysis compared the difference in FAM19A5 expression between the RSSI group and
150   healthy controls, while multivariable linear regression analysis compared the correlation between
151   FAM19A5 and the infarct volume. In order to verify the correlation between the imaging
152   characteristics of total MRI burden and FAM19A5, we first determined the confounding factors
153   by univariate logistic analysis, and those with P-value <0.1 were included in multivariable logistic
154   analysis for adjustment. Due to the high incidence of WMH and EPVS, the variables were
155   classified into different grades that were analyzed by multivariate ordinal logistic regression. Next,
156   lacune and CMB were analyzed by multivariate binary logistic regression with the classification
157   into the presence and absence. Deep and lobar CMB and, as well as PVWMH and DWMH were
158   independently analyzed by multivariate logistics. P<0.05 was considered statistically significant.
159   In the RSSI group, the correlation between FAM19A5 levels and clinical scales (NIHSS scale at
160   NIHSS scale at admission, NIHSS scale at 14 days, ΔNIHSS, percentage of NIHSS improvement,
161   and total MRI burden of cSVD) were assessed, in which Spearman's test performed the
162   comparisons between continuous variables. All statistical analyses were performed using IBM
163   SPSS Statistics for Windows, version 26.0 (IBM Corporation, Armonk, NY, USA).

164

3. Results

3.1. Recruitment and baseline characteristics of subjects

A total of 609 subjects were selected in our study from 1784 RSSI patients and healthy individuals from May 2018 to June 2020 (Figure 1). There were 1342 acute infarction patients were included in the filter process; among them, 573 patients with severe large artery stenosis and occlusion were excluded, and 188 patients were excluded because of cardiac diseases or other diseases that may lead to cerebral infarctions. Finally, 344 RSSI patients were included in the current study, the mean age was 61.874±11.359 years, and 211 (63.2%) patients were males. Also, 265 healthy controls were strictly filtered from 541 patients undergoing health checkups, the mean age was 61.411±11.978 years, and 115 (43.4%) patients were males (Table 1).

3.2. FAM19A5 level and infarct volume of RSSI

The current study showed a positive correlation between FAM19A5 and recent small subcortical infarct. Mean±standard deviation of serum FAM19A5 in the RSSI and healthy control groups was 681.894±1225.014 and 432.582±777.871 pg/mL, respectively (Figure 2). After adjustment for age, sex, hypertension, diabetes, smoking, pulse, triglyceride, cholesterol, low-density lipoprotein, and glucose, our results showed that the expression of FAM19A5 was higher in the RSSI group than the control group (odds ratio (OR) (95% confidence interval (CI))=1.265 (1.032–1.549), P=0.023). The linear regression analysis of infarct persons showed the correlation between infarct volume and FAM19A5 (OR (95% CI)= 1.587 (1.324–1.901), P<0.001) (Table 2).

3.3. FAM19A5 and imaging characteristics of total MRI burden

Serum FAM19A5 levels in imaging characteristics of cSVD total MRI burden are depicted in Figure 3. A positive correlation between the total MRI burden of cSVD and FAM19A5 levels was established (P=0.041) and assessed by univariate and multivariable regression analysis. (Table 3) Age, sex, hypertension, diabetes, smoking, drinking, pulse, blood pressure, volume of cerebral infarction, glucose, C-reactive protein, triglyceride, total cholesterol, low-density lipoprotein, high-density lipoprotein, white blood cell count, uric acid, and homocysteine were included in the adjustment process.

After adjustment for age, hypertension, pulse, systolic blood pressure, total cholesterol, low-density lipoprotein, C-reactive protein, and high sensitivity C-reactive protein, multivariate ordinal logistic regression analysis showed a positive correlation between FAM9A5 and white matter hypertension on Fazekas scale (OR (95% CI)=1.842 (1.459–2.326), P<0.001). (Table 3) Our further analysis showed that FAM19A5 was correlated with both periventricular white matter hypertensity (OR (95% CI)= 1.560 (1.311–1.855), P<0.001) and deep white matter hypertensity (OR (95% CI)= 1.557 (1.268–1.910), P<0.001).

199 After adjustment for age, sex, hypertension, smoking, total cholesterol, and low-density
200 lipoprotein, multivariate ordinal logistic regression analysis showed a positive correlation between
201 FAM9A5 and EPVS Potter scale (OR (95% CI)= 1.434 (1.211–1.698), P<0.001).

202 The current study did not identify any significant correlation between FAM9A5 and the presence
203 or absence of lacunae (OR (95% CI)= 0.980 (0.801–1.199), P=0.844) and CMB (OR (95% CI)=
204 0.895 (0.659–1.216), P=0.479). We also found that deep microhemorrhage and cortical
205 microhemorrhage were not related to the FAM19A5 level.

206 **3.4. Correlation between FAM19A5 and outcomes**

207 The mean±SD of NIHSS at admission, NIHSS at 14 days, and ΔNIHSS was 3.22±2.88, 2.52±2.66,
208 and 0.69±1.27, respectively, and the mean±SD of the percentage of NIHSS improvement was
209 25.4±48.5. Spearman's correlation analysis demonstrated that the FAM19A5 level was not
210 significantly correlated with NIHSS at admission and 14 days after admission. However, it was
211 positively correlated with ΔNIHSS (P=0.031) and the percentage of NIHSS improvement
212 (P=0.011) (Table 4).

213

214 4. Discussion

215 The results showed that FAM19A5 increased in the RSSI group, showing a positive correlation
216 with cerebral infarction volume. The multivariate logistic analysis showed that the level of
217 FAM19A5 was positively correlated with the total MRI burden of cSVD, which might be
218 effectuated through the correlation with WMH and EPVS. Moreover, FAM19A5 suggested a
219 better outcome for RSSI patients. By combining the laboratory biomarker with clinical and
220 imaging findings, we verified the association of FAM19A5 with the severity of cSVD and its
221 prognosis, which might guide the treatment of cerebral small vessel diseases.

222 Reportedly, FAM19A5 participates in nervous system development at an early stage. It is
223 expressed in neurons, oligodendrocyte precursor cells (OPCs), astrocytes, and microglia and is
224 involved in the OPC-mediated repair process as an acute inflammatory factor after pathological
225 brain injury (Shahapal et al. 2019). Previous studies have shown that FAM19A5 increases the level
226 of pro-inflammatory cytokines and participates in the TNF-α-induced inflammatory response in
227 the hypothalamus, which also confirms the role of FAM19A5 in acute inflammation (Kang et al.
228 2020). A clinical study demonstrated that FAM19A5 was increased in neuromyelitis optica
229 spectrum disorders, the reason may be that after central nervous system (CNS) injury, FAM19A5
230 is secreted by reactive astrocytes, which triggers excessive proliferation of neuroglial cells and
231 participates in the proliferation of reactive gliosis (Lee et al. 2019). Not only acute injury, but also
232 FAM19A5 is involved in the pathophysiological process of chronic inflammation. As a bridge

233   connecting chronic inflammation, reactive gliosis, and degenerative diseases in the brain,
234   FAM19A5 is overexpressed in severe depressive disorder and negatively correlated with cortical
235   thickness. It is also highly expressed in Alzheimer's in genetic studies and vascular dementia (Han
236   et al. 2020; Li et al. 2020; Mez et al. 2017).

237   Microglia and astrocytes are activated in acute infarction, leading to high expression of
238   inflammatory factors via damage-associated molecular pattern (DAMPs) and "inflammatory
239   waterfall" however, the correlation between FAM19A5 and RSSI has not yet been realized (Chen
240   & Nuñez 2010). To the best of our knowledge, we assessed the expression of FAM19A5 in cSVD
241   and found that the expression level of FAM19A5 in RSSI patients was high and correlated with
242   the infarct volume of RSSI. Based on the previous studies, we speculated that the reasons for the
243   increased expression of FAM19A5 after cerebral infarction might be as follows: FAM19A5 is
244   secreted by reactive glial cells and is involved in OPC-mediated repair process, triggers glial cell
245   proliferation, and glial scar formation. This phenomenon is confirmed by the correlation between
246   FAM19A5 and cerebral infarction volume: a large volume of brain injury indicates severe nerve
247   damage and acute inflammation. Also, higher FAM19A5 predicted a larger ΔNIHSS and
248   percentage of NIHSS improvement, suggesting that FAM19A5 contributes to the repair process
249   of the nervous system via OPC-mediated gliosis and nerve repair process, thereby improving the
250   stroke prognosis.

251   The mechanism of cerebral small vessel disease is complex, and the pathogenesis varies in imaging
252   characteristics of cSVD and in different areas of the brain (Blanco et al. 2017). Deep CMB is
253   closely related to hypertension, and lobar CMB might be caused by cerebral vascular amyloidosis
254   (Ding et al. 2015; Poels et al. 2010; Wardlaw et al. 2013a). Several studies have shown that high
255   signal intensity in white matter is correlated with the overexpression of various inflammatory
256   factors (Satizabal et al. 2012). The disturbance of cerebrospinal fluid circulation in perivascular
257   space or the imbalance of aquaporin in astrocytes might be one of the causes of EPVS. In addition,
258   histopathological studies have shown that PVS is consistent with the location of inflammatory
259   infiltration in EPVS (Kwee & Kwee 2007). Lacune is usually considered to be transformed from
260   other lesions (Wardlaw et al. 2013a; Wardlaw et al. 2019). Our correlation analysis results
261   suggested that higher FAM19A5 levels reflect a severe total MRI burden, and multivariate logistic
262   analysis showed that FAM19A5 reflects the severity of WMH and EPVS. Comprehensively, we
263   speculated that the correlation between FAM19A5 and total MRI burden could be attributed to the
264   effects on WMH and EPVS, which might be due to the involvement of FAM19A5 in chronic
265   inflammation in the brain. Since WMH and EPVS are related to chronic and persistent
266   inflammatory responses, the expression and activity of many inflammatory markers are elevated
267   (Blanco et al. 2017; Kwee & Kwee 2007; Satizabal et al. 2012). Herein, we did not find any
268   correlation between deep or lobar CMB and FAM19A5. Comprehensively, the reason may be that
269   CMBs are related to hypertension or amyloidosis, reflecting the deposition of hemosiderin in

270 macrophages and failing to reflect the persistent inflammatory response of the brain (Janaway et
271 al. 2014). In addition, lacunae are usually thought to be transformed from other lesions, and it is
272 complex to trace encephalomalacia to its origins. Therefore, the etiology and mechanism are
273 complex and lack solid evidence. Taken together, FAM19A5 is used as a chronic inflammatory
274 factor that participates in the progression of cSVD and reflects its severity.

275 Nevertheless, the present study has several limitations. Firstly, because of our strict screening of
276 patients with cerebral infarction, the study included only a small number of cases, and the various
277 examination strategies of subcenters refer to insufficient tests in SWI examinations, thereby
278 limiting the CMB research. Secondly, our subjects are homogeneous, and most of them are Han
279 people in northern China. This problem could be solved by increasing the number of patients in
280 the future. Thirdly, severe large artery stenosis was defined as stenosis >50% of a carotid or
281 intracranial artery according to TOAST, it is the most broadly used but may leading to the
282 insufficient exclusion of those with a high carotid plaque burden. Other classification systems like
283 SPARKLE and CISS is meaningful in solving this problem in the future.(Bogiatzi et al. 2014;
284 Zhang et al. 2019) Finally, due to the limitations of the cross-sectional analysis, we are unable to
285 study causality. Thus, additional studies and dynamic observation are needed to solve this problem
286 in the future.

287 In summary, FAM19A5 reflects the severity of RSSI and predicts a promising prognosis as an
288 acute inflammatory factor. In the imaging characteristics of cSVD, FAM19A5 can reflect the
289 severity of WMH and EPVS. That might guide the diagnosis and treatment of cerebrovascular
290 diseases.

291

292

Declaration of Competing Interests

294 None.

295

Acknowledgments

297 We gratefully acknowledge the assistance of the Institute of Cerebrovascular Diseases Cooperative
298 Medical Institutions for clinical support.

299

Ethical Statement

301 The trial was conducted in accordance with the Declaration of Helsinki (as revised in 2013). The
302 study was approved by the Ethics Review Board of the Affiliated Hospital of Qingdao University
303 (QYFY WZLL 26787) and informed consent was taken from all individual participants.

304

305

306 # References:

307 Blanco PJ, Müller LO, and Spence JD. 2017. Blood pressure gradients in cerebral arteries: a clue to pathogenesis
308   of cerebral small vessel disease. *Stroke and vascular neurology* 2:108-117. 10.1136/svn-2017-000087
309 Bogiatzi C, Wannarong T, McLeod AI, Heisel M, Hackam D, and Spence JD. 2014. SPARKLE (Subtypes of
310   Ischaemic Stroke Classification System), incorporating measurement of carotid plaque burden: a new
311   validated tool for the classification of ischemic stroke subtypes. *Neuroepidemiology* 42:243-251.
312   10.1159/000362417
313 Cannistraro RJ, Badi M, Eidelman BH, Dickson DW, Middlebrooks EH, and Meschia JF. 2019. CNS small vessel
314   disease: A clinical review. *Neurology* 92:1146-1156. 10.1212/WNL.0000000000007654
315 Chen GY, and Nuñez G. 2010. Sterile inflammation: sensing and reacting to damage. *Nature reviews Immunology*
316   10:826-837. 10.1038/nri2873
317 Ding J, Sigurdsson S, Garcia M, Phillips CL, Eiriksdottir G, Gudnason V, van Buchem MA, and Launer LJ. 2015.
318   Risk Factors Associated With Incident Cerebral Microbleeds According to Location in Older People:
319   The Age, Gene/Environment Susceptibility (AGES)-Reykjavik Study. *JAMA neurology* 72:682-688.
320   10.1001/jamaneurol.2015.0174
321 Gattringer T, Eppinger S, Pinter D, Pirpamer L, Berghold A, Wünsch G, Ropele S, Wardlaw JM, Enzinger C, and
322   Fazekas F. 2015. Morphological MRI characteristics of recent small subcortical infarcts. *International*
323   *journal of stroke : official journal of the International Stroke Society* 10:1037-1043. 10.1111/ijs.12499
324 Han K-M, Tae W-S, Kim A, Kang Y, Kang W, Kang J, Kim Y-K, Kim B, Seong JY, and Ham B-J. 2020. Serum FAM19A5
325   levels: A novel biomarker for neuroinflammation and neurodegeneration in major depressive
326   disorder. *Brain, behavior, and immunity* 87:852-859. 10.1016/j.bbi.2020.03.021
327 Janaway BM, Simpson JE, Hoggard N, Highley JR, Forster G, Drew D, Gebril OH, Matthews FE, Brayne C, Wharton
328   SB, Ince PG, Function MRCC, and Ageing Neuropathology S. 2014. Brain haemosiderin in older people:
329   pathological evidence for an ischaemic origin of magnetic resonance imaging (MRI) microbleeds.
330   *Neuropathol Appl Neurobiol* 40:258-269. 10.1111/nan.12062
331 Kang D, Kim HR, Kim KK, Kim DH, Jeong B, Jin S, Park JW, Seong JY, and Lee BJ. 2020. Brain-specific chemokine
332   FAM19A5 induces hypothalamic inflammation. *Biochem Biophys Res Commun* 523:829-834.
333   10.1016/j.bbrc.2019.12.119
334 Kwee RM, and Kwee TC. 2007. Virchow-Robin spaces at MR imaging. *Radiographics : a review publication of the*
335   *Radiological Society of North America, Inc* 27:1071-1086.
336 Lee HL, Seok HY, Ryu H-W, Cho EB, Kim BC, Kim BJ, Min J-H, Seok JM, Shin HY, Kang S-Y, Kwon O-H, Lee S-S, Oh
337   J, Sohn E-H, Huh S-Y, Cho J-Y, Seong JY, and Kim B-J. 2019. Serum FAM19A5 in neuromyelitis optica

338   spectrum disorders: Can it be a new biomarker representing clinical status? *Multiple sclerosis*
339   *(Houndmills, Basingstoke, England)*:1352458519885489. 10.1177/1352458519885489

340   Li J, Li S, Song Y, Zhou W, Zhu X, Xu S, Ma Y, and Zhu C. 2020. Association of Serum FAM19A5 with Cognitive
341   Impairment in Vascular Dementia. *Dis Markers* 2020:8895900. 10.1155/2020/8895900

342   Li XN, Hao DP, Qu MJ, Zhang M, Ma AB, Pan XD, and Ma AJ. 2021. Development and Validation of a Plasma
343   FAM19A5 and MRI-Based Radiomics Model for Prediction of Parkinson's Disease and Parkinson's
344   Disease With Depression. *Frontiers in neuroscience* 15:795539. 10.3389/fnins.2021.795539

345   Mez J, Chung J, Jun G, Kriegel J, Bourlas AP, Sherva R, Logue MW, Barnes LL, Bennett DA, Buxbaum JD, Byrd GS,
346   Crane PK, Ertekin-Taner N, Evans D, Fallin MD, Foroud T, Goate A, Graff-Radford NR, Hall KS, Kamboh
347   MI, Kukull WA, Larson EB, Manly JJ, Haines JL, Mayeux R, Pericak-Vance MA, Schellenberg GD, Lunetta
348   KL, and Farrer LA. 2017. Two novel loci, COBL and SLC10A2, for Alzheimer's disease in African
349   Americans. *Alzheimers Dement* 13:119-129. 10.1016/j.jalz.2016.09.002

350   Poels MMF, Vernooij MW, Ikram MA, Hofman A, Krestin GP, van der Lugt A, and Breteler MMB. 2010. Prevalence
351   and risk factors of cerebral microbleeds: an update of the Rotterdam scan study. *Stroke* 41:S103-S106.
352   10.1161/STROKEAHA.110.595181

353   Potter GM, Chappell FM, Morris Z, and Wardlaw JM. 2015. Cerebral perivascular spaces visible on magnetic
354   resonance imaging: development of a qualitative rating scale and its observer reliability.
355   *Cerebrovascular diseases (Basel, Switzerland)* 39:224-231. 10.1159/000375153

356   Satizabal CL, Zhu YC, Mazoyer B, Dufouil C, and Tzourio C. 2012. Circulating IL-6 and CRP are associated with
357   MRI findings in the elderly: the 3C-Dijon Study. *Neurology* 78:720-727.
358   10.1212/WNL.0b013e318248e50f

359   Shahapal A, Cho E, Yong H, Jeong I, Kwak H, Lee J, Kim W, Kim B, Park H, Lee W, Kim H, Hwang J, and Seong J.
360   2019. FAM19A5-LacZFAM19A5 Expression During Embryogenesis and in the Adult Traumatic Brain
361   of Knock-in Mice. *Frontiers in neuroscience* 13:917. 10.3389/fnins.2019.00917

362   Sims JR, Gharai LR, Schaefer PW, Vangel M, Rosenthal ES, Lev MH, and Schwamm LH. 2009. ABC/2 for rapid
363   clinical estimate of infarct, perfusion, and mismatch volumes. *Neurology* 72:2104-2110.
364   10.1212/WNL.0b013e3181aa5329

365   Tom Tang Y, Emtage P, Funk WD, Hu T, Arterburn M, Park EEJ, and Rupp F. 2004. TAFA: a novel secreted family
366   with conserved cysteine residues and restricted expression in the brain. *Genomics* 83:727-734.

367   Wardlaw JM, Smith C, and Dichgans M. 2013a. Mechanisms of sporadic cerebral small vessel disease: insights
368   from neuroimaging. *The Lancet Neurology* 12:483-497. 10.1016/S1474-4422(13)70060-7

369   Wardlaw JM, Smith C, and Dichgans M. 2019. Small vessel disease: mechanisms and clinical implications. *The*
370   *Lancet Neurology* 18:684-696. 10.1016/S1474-4422(19)30079-1

371   Wardlaw JM, Smith EE, Biessels GJ, Cordonnier C, Fazekas F, Frayne R, Lindley RI, O'Brien JT, Barkhof F,
372   Benavente OR, Black SE, Brayne C, Breteler M, Chabriat H, Decarli C, de Leeuw F-E, Doubal F, Duering
373   M, Fox NC, Greenberg S, Hachinski V, Kilimann I, Mok V, Oostenbrugge Rv, Pantoni L, Speck O, Stephan
374   BCM, Teipel S, Viswanathan A, Werring D, Chen C, Smith C, van Buchem M, Norrving B, Gorelick PB, and
375   Dichgans M. 2013b. Neuroimaging standards for research into small vessel disease and its contribution
376   to ageing and neurodegeneration. *The Lancet Neurology* 12:822-838. 10.1016/S1474-
377   4422(13)70124-8

378   Zhang H, Li Z, Dai Y, Guo E, Zhang C, and Wang Y. 2019. Ischaemic stroke etiological classification system: the

379   agreement analysis of CISS, SPARKLE and TOAST.   4:123-128. 10.1136/svn-2018-000226

380

Table 1: Baseline characteristics of RSSI group and healthy controls

SBP: systolic blood pressure, DBP: diastolic blood pressure, FAM19A5: family with sequence similarity 19 memberA5

	RSSI (n=334)	Healthy control (n=265)
Age, years (SD)	61.874±11.359	61.411 (11.978)
Sex, male (n%)	211 (63.173)	115 (43.396)
hypertension, n (n%)	207 (61.976)	131 (49.434)
Diabetes, n (n%)	90 (27.245)	44 (16.604)
Current smoking, n (n%)	121 (36.228)	33 (13.415)
Pulse, beats/min (IQR)	68 (59–77)	69 (63–76)
SBP, mmHg (IQR)	151 (137–167)	133 (120–149)
DBP, mmHg (IQR)	84 (76–95)	76 (68–84)
FAM19A5, ng/mL(SD)	0.682±1.225	0.433±0.778

Table 2: Correlation between FAM19A5 and RSSI with its infarct volume

a: Adjusted for age, sex, hypertension, diabetes, current smoking, pulse, triglyceride, cholesterol, low-density lipoprotein, glucose .

b: Binary logistic regression analysis of FAM19A5 level between RSSI group and heathy controls.

c: Linear regression analysis of FAM19A5 level and infarct volume of RSSI patients. R^2=0.094.

Bold indicates statistically significant P-values (P<0.05)

| | | Unadjusted | | Adjusted[a] | |
		OR (95% CI)	P-value	OR (95% CI)	P-value
Model 1[b]					
RSSI group *vs.* healthy controls		1.029 (1.077–1.559)	**0.006**	1.265 (1.032–1.549)	**0.023**
Model 2[c]					
FAM19A5 and infarct volume		1.597 (1.339–1.906)	**<0.001**	1.587 (1.324–1.901)	**<0.001**

Table 3: Correlation between FAM19A5 and characteristics of cSVD total MRI burden

WMH, EPVS, and total MRI burden underwent ordinal logistic regression, Lacune and CMB were assessed by binary logistic regression.

a: Adjusted for age, hypertension, pulse, SBP, TC, LDL, CRP, and hsCRP.

b: Adjusted for age, sex, hypertension, smoking, TC, and LDL.

c: Adjusted for age, hypertension, SBP, and Hcy.

d: Adjusted for glucose, TC, and UA.

e: Adjusted for age, SBP, glucose, TC, LDL, CRP, and Hcy

SBP: systolic blood pressure , TC: total cholesterol , LDL: low-density lipoprotein , Hcy: homocysteine, CI volume: cerebral infarction volume, CRP: C-reactive protein , hsCRP: high sensitivity C-reactive protein .

Bold indicates statistically significant P-values (P<0.05).

		Unadjusted			Adjusted	
☐	☐	OR (95% CI)	P-value	☐	OR (95% CI)	P-value
WMH[a]						
Fazekas scale		1.697 (1.408–2.044)	**<0.001**		1.842 (1.459–2.326)	**<0.001**
EPVS[b]						
Potter scale		1.430 (1.213–1.687)	**<0.001**		1.434 (1.211–1.698)	**<0.001**
Lacune[c]						
Presence or absence		0.913 (0.765– 1.89)	0.311		0.980 (0.801–1.199)	0.844
CMB[d]						
Presence or absence		0.917 (0.683–1.232)	0.567		0.895 (0.659–1.216)	0.479
cSVD[e]						
Total MRI burden		1.183 (1.011-1.384)	**0.036**		1.251(1.010-1.550)	**0.041**

Table 4: Association of FAM19A5 levels with clinical scales of patients

NIHSS: National Institutes of Health stroke scale.

Bold indicates statistically significant P-values (P<0.05).

	RSSI (n=334)	P-value
NIHSS scale at admission	3.2173±2.881	0.869
NIHSS scale at 14 days	2.524±2.657	0.109
ΔNIHSS	0.693±1.269	**0.031**
Percentage of NIHSS improvement, %	25.361±48.454	**0.011**

Figure 1

Figure 1: Recruitment flowchart.
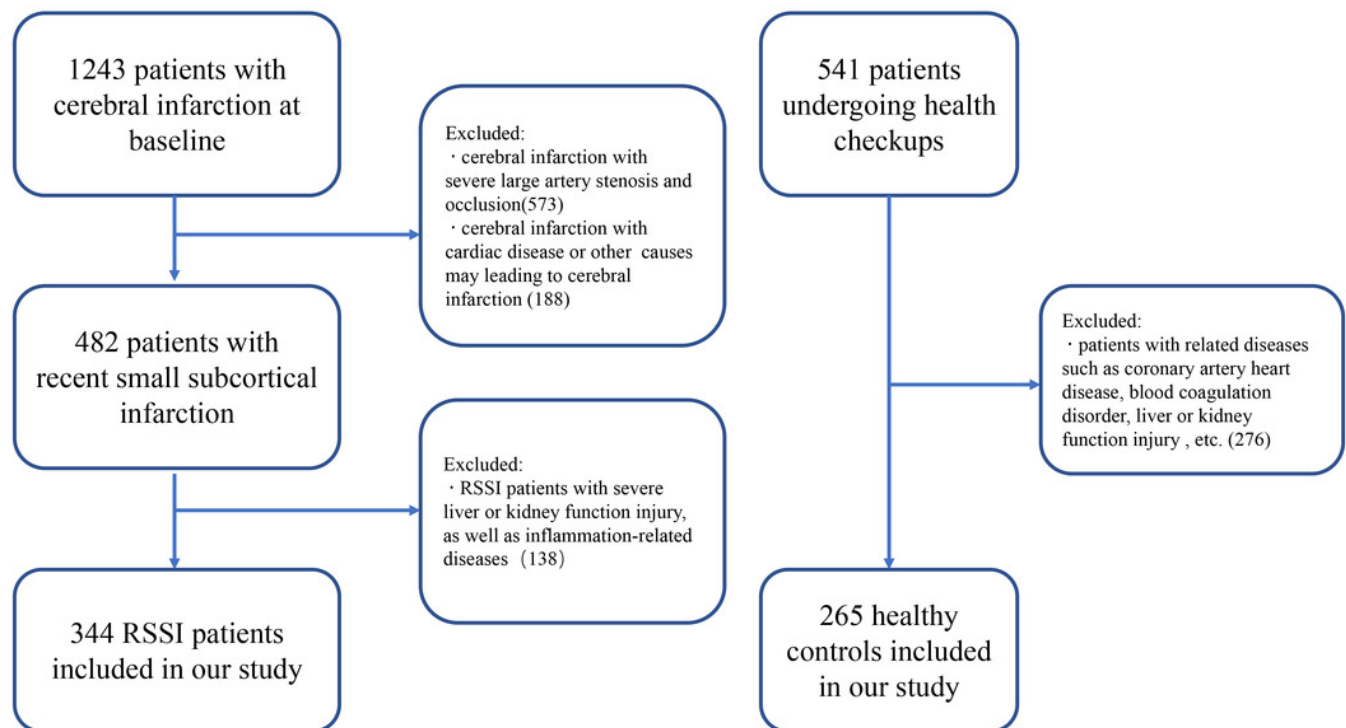
Figure 2

Figure 2: FAM19A5 levels of RSSI group &healthy control

Serum level of FAM19A5 (ng/mL) in the RSSI group (mean ± SD= 0.682 ± 1.225) is higher than in healthy control (mean ± SD= 0.433 ± 0.778), P-value = 0.023.

Manuscript to be reviewed

FAM19A5 levels of RSSI group & healthy control
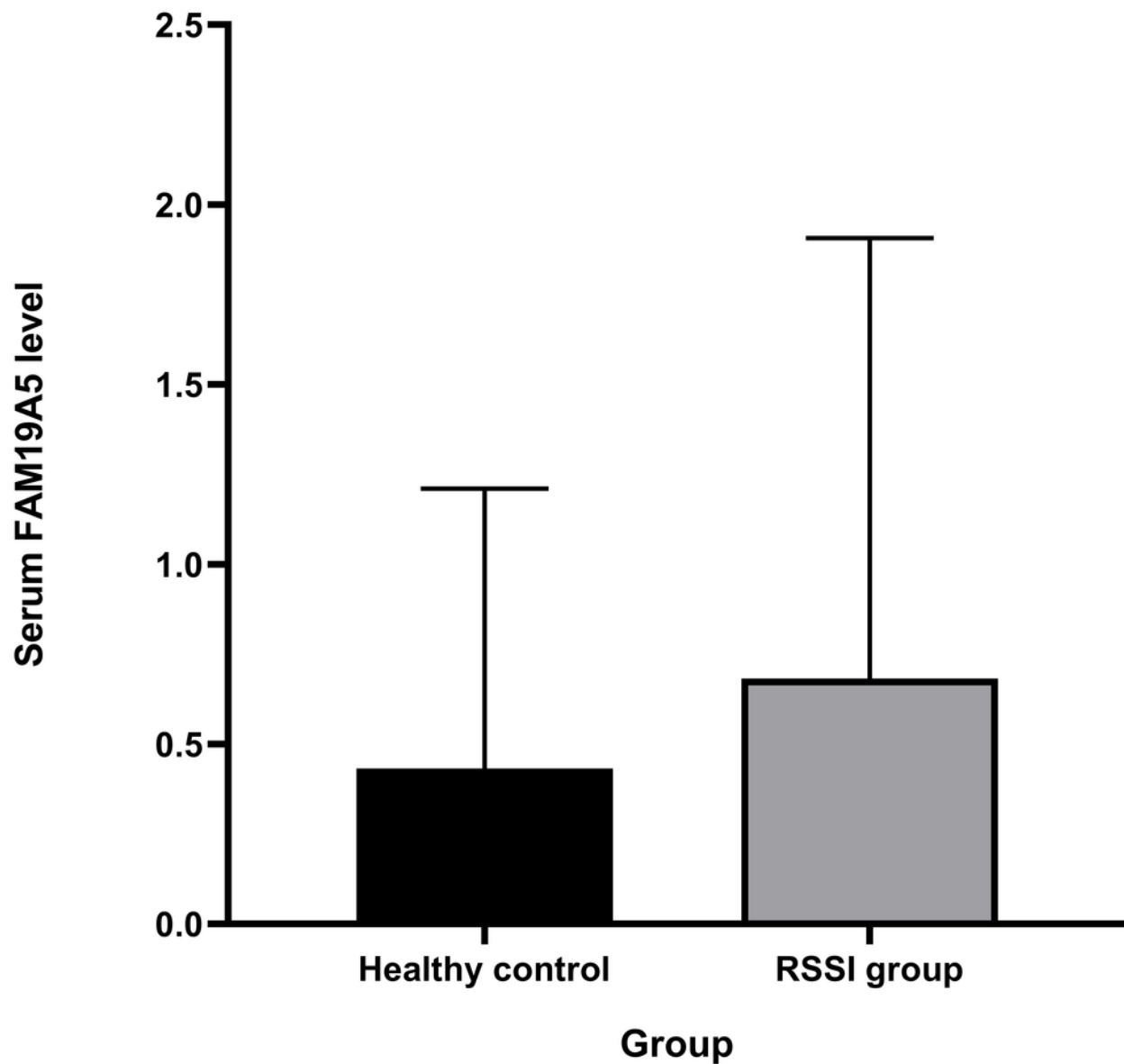
Figure 3

Figure 3: Level of FAM19A5 and imaging characteristics of total MRI burden

Figure 3: Level of FAM19A5 and imaging characteristics of total MRI burden. (ng/mL)

FAM19A5 level in persons with Fazekas scale 0, 1, 2, and 3: 0.144±0.056, 0.415±0.814, 0.745±1.211, and 1.761±2.001, respectively. (n= 4, 182, 116, and 42, respectively. P<0.001)

FAM19A5 level in persons with Potter scale 1, 2, 3, and 4: 0.276±0.564, 0.751±1.392, 1.065±1.423, and 1.0162±1.388, respectively. (n= 114, 122, 84, and 24, respectively. P<0.001)

FAM19A5 level in persons without or with Lacune: 0.777±1.372 and 0.635±1.134, respectively. (n=125 and 219, P=0.844)

FAM19A5 level in persons without or with CMB: 0.736±1.395 and 0.614±0.870, respectively. (n=95 and 51, P=0.479)

CMB=cerebral microbleed; EPVS=enlarged perivascular space; WMH=white matter hyperintensity.

Bold indicates statistically significant P-values (P<0.05). FAM19A5 level was described as mean±standard deviation.